MARS PARKING ORBIT SELECTION

by
Prasun N. Desai*
The George Washington University
NASA Langley Research Center
and
Robert D. Braun**
NASA Langley Research Center

ABSTRACT

For a Mars mission, the selection of a parking orbit is greatly influenced by the precession caused by the oblateness of the planet. This affects the departure condition for Earth return, and therefore, the mass required in low-Earth orbit (LEO) for a Mars mission. In this investigation, minimum LEO mass penalties were observed for parking orbits characterized by having near-equatorial inclinations, high eccentricities, and requiring a three-dimensional departure burn. However, because near-equatorial inclination orbits have poor planetary coverage characteristics, they are not desirable from a science viewpoint. To enhance these science requirements along with landing site accessibility, a penalty in mission performance (initial LEO mass) is required. This study shows that this initial LEO mass penalty is reduced for orbits characterized with low to moderate eccentricities, non-equatorial inclinations, and a tangential periapsis arrival and departure burn. This investigation also shows that the use of retrograde orbits (inclinations above 90°) can reduce the penalty in mission performance. Finally, for a particular mission, the selection of a final Mars parking orbit cannot be based purely on mission performance. A tradeoff between mission performance, science requirements, and landing site accessibility needs to be made.

INTRODUCTION

As demonstrated by President Bush's speech at the 20th anniversary of the Apollo Moon Landing and by the Sally Ride Report "Leadership and America's Future in Space," there has been renewed interest for a manned mission to Mars in the early 21st century (2010-2025). Recent studies have shown that numerous opportunities exist for a chemically propelled, high-thrust vehicle to perform a 1-2-year round-trip mission which includes a 60-day stopover.[1,2,3] Although a great deal of work has been directed toward determining optimum interplanetary trajectories for an Earth-Mars manned mission, less effort has been devoted to the determination of an appropriate Mars parking orbit. Therefore, the primary focus of this investigation is to determine the effects of Mars parking orbit selection on the mission profile. In particular, parking orbit selection dictates the propulsive requirements necessary for injection into and departure from Mars orbit and may result in a 30-50 percent variation in the initial LEO mass.[4]

The objective of this investigation is to identify trends and aspects of Mars parking orbits for an initial manned mission. Parking orbit selection requires a thorough analysis of the following parameters: (1) periapsis altitude, (2) inclination, (3) eccentricity, (4) length of stopover, (5) scientific requirements, and (6) landing site accessibility. The effects of orbital precession resulting from the oblateness of Mars greatly influence the orbit selection process. This paper addresses the impacts of each of these issues.

NOMENCLATURE

altp	periapsis altitude, km
e	eccentricity
i	inclination, deg
$\vec{I}, \vec{J}, \vec{K}$	unit vectors
Isp	specific impulse, sec
J_n	zonal coefficient
L	geocentric latitude, deg
LEO	low-Earth orbit
LH_2	liquid hydrogen
LOX	liquid oxygen
M	mass, kg
MEM	mission excursion module

*JIAFS Research Engineer, Member AIAA.
**Aerospace Engineer, Space Systems Division, Member AIAA.

M_i/M_f	ratio of initial mass to final mass
P_n	Legendre polynomial
POST	Program to Optimize Simulated Trajectories
r	position of spacecraft, m
r_e	equatorial radius, m
SOI	sphere of influence
Sol	solar day
SWISTO	Swingby-Stopover Optimization Program
T/W	ratio of thrust to weight
3-D	3-dimensional
t	time
U	gravitational potential
$\vec{V}_\infty$	hyperbolic excess velocity, km/sec
α	right ascension, deg
β	out-of-plane component of the departure burn direction, deg
δ	declination, deg
ΔV	velocity increment, km/sec
ΔV_{dept}	velocity increment at departure, km/sec
ΔV_{ins}	velocity increment at insertion, km/sec
γ	in-plane component of the departure burn direction, deg
μ	gravitational parameter, m^3/sec^2
θ	true anomaly, deg

ANALYSIS

Vehicle Characteristics and Mission Scenario

The baseline vehicle and interplanetary mission profile are based on the requirements of an initial manned exploration scenario.[1,2,3] The interplanetary transfer vehicle's mass breakdown was obtained from Refs. 5 and 6 and is given in Table 1. Note that a range of mission excursion module (MEM) masses are given for the various parking orbit requirements. In this study, a LOX/LH_2 rocket engine with a vacuum specific impulse (Isp) of 480 seconds is utilized and the corresponding tankage mass is assumed to be 10 percent of the propellant mass.

Table 1
Vehicle Dry Mass Estimate

Vehicle Component	Mass, kg
Two habitation modules[5]	43,200
Truss structure and support equipment[5]	11,000
Earth return capsule[6]	6,800
MEM	34,000-82,400
Total $mass_{Mars\ arrival}$	95,000-143,400
Total $mass_{Mars\ departure}$	61,000
Total $mass_{Earth\ arrival}$	6,800

Because the entire analysis is performed through a series of mass ratio calculations, the results presented are applicable to any vehicle design provided that three parameters remain roughly constant: (1) the propulsion systems must be similar (in terms of Isp and tank structure), (2) the ratio of mass left behind at Mars to Earth return payload must be comparable, and (3) the use of an impulsive velocity addition is valid. The mass ratio (M_i/M_f) represents the mass (kg) that must be placed into LEO for every kilogram of mass returned to LEO at the end of the mission. For example, the vehicle described in the analysis has a mass of $6.8x10^3$ kg at Earth return. Thus, a M_i/M_f of 150 would require an initial LEO mass of $1.02x10^6$ kg.

The mission begins with the interplanetary vehicle departing from the space station in LEO. Upon arrival at Mars, a tangential burn is performed at periapsis of the approach hyperbola for insertion of the vehicle into a parking orbit (Fig. 1a). Following circularization at periapsis altitude, the MEM descends to the Martian surface (Fig. 1b). After performing the necessary excursion operations, the MEM ascends to a phasing orbit, where an apoapsis burn is performed so rendezvous with the orbiter can occur in the parking orbit (Fig. 1c). At the end of the 60-day stopover, the MEM is discarded, and a departure burn is performed for Earth return (Fig. 1d). Upon Earth arrival, the habitation modules and support structure are discarded, and only the manned capsule is returned to the space station. Note that the appropriate propellant tankage is discarded after performing each burn.

The analysis was performed for the following interplanetary mission profile:

Earth departure:	April 5, 2017
Venus swingby:	September 10, 2017
Mars arrival:	March 24, 2018
Mars departure:	May 23, 2018
Earth return:	November 15, 2018

This profile is a typical opposition class mission taken from the set of opportunities presented in Ref. 1, which includes a Venus swingby on the outbound (Earth-Mars) trajectory leg and has a total trip time of 1.6 years. For this mission profile, the ΔV values for Earth departure and return are 4.17 km/sec and 1.13 km/sec, respectively. Upon Mars arrival, the inbound and out-

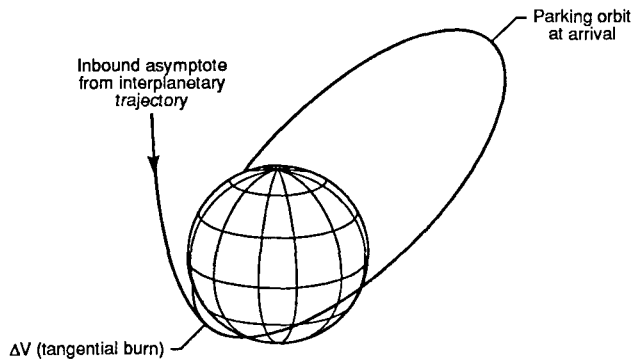

a. Mars arrival.

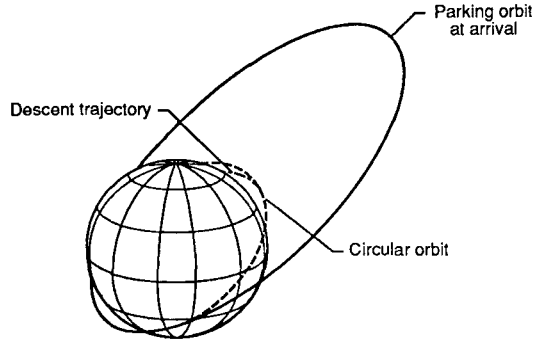

b. Mars descent.

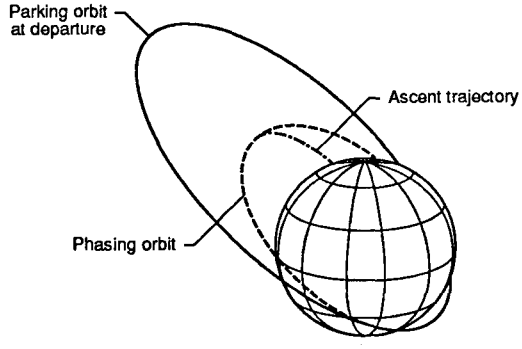

c. Mars ascent.

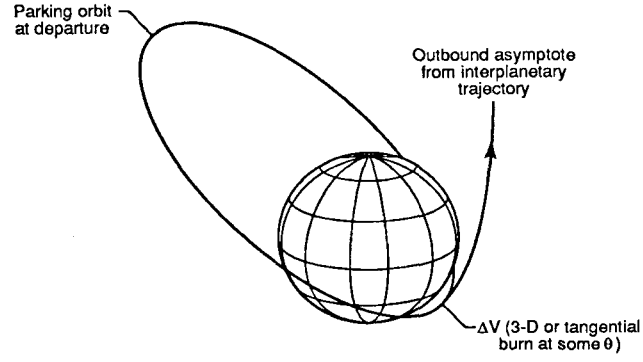

d. Mars departure.

Fig. 1. Mission geometry.

bound hyperbolic velocity vectors can be described in terms of a right ascension (α), declination (δ), and hyperbolic excess velocity ($\vec{V}_\infty$) presented in the following table:

Inbound	Outbound
$\alpha = 253.99°$	$\alpha = 212.57°$
$\delta = -21.4°$	$\delta = -12.5°$
$\lvert\vec{V}_\infty\rvert = 5.441$ km/sec	$\lvert\vec{V}_\infty\rvert = 3.873$ km/sec

These interplanetary transfer, arrival, and departure conditions were obtained using a patch-conic approach. As a result of the patch-conic two-body approximation, the position vector at the sphere of influence (SOI) is not uniquely defined. Therefore, numerous parking orbit inclinations may be achieved. However, the maximum declination (δ_{max}) between the inbound and outbound velocity vectors limits the achievable parking orbit inclination.[7] That is, the achievable range of orbital inclinations (i) is

$$|\delta_{max}| \leq i \leq 180° - |\delta_{max}|$$

If inclinations beyond this range are desired, an additional propulsive maneuver is required. For this mission profile, an inclination range between 21.5° and 158.5° was possible. For eccentricity, an upper limit on the period of the parking orbit of one Martian day (1 Sol) was imposed because of concerns that for an orbit with a longer period, the MEM would approach escape velocity during ascent and rendezvous. The various inclinations (i) and eccentricities (e) considered in the parametric portion of this analysis were

i = 21.5°, 40°, 60°, 75°, 90°, 105°, 125°, 145°, 158.5°
e = 0.05, 0.25, 0.50, 0.75, 1 Sol orbit

This analysis was performed for periapsis altitudes of 250 km and 500 km. These altitudes were selected for consistency with sizing and mass estimates of the MEM subsystems.[8]

In this analysis, a parametric study was first performed, where the inclination and eccentricity were varied to determine the ΔV values for Mars insertion and departure. In this manner, trends of initial LEO mass versus inclination and eccentricity were developed. Secondly, an "exact precession orbit" was sought. This is defined as a parking orbit which would precess in such a way that at the end of the stopover, a tangential periapsis burn could be performed at depar-

ture (Fig. 1d). In the parametric study, a specific inclination and eccentricity of the parking orbit were targeted from the inbound interplanetary asymptote at the SOI. After the 60-day stopover, a three-dimensional departure burn was utilized at periapsis in order to achieve the outbound hyperbolic asymptote requirements. For the exact precession study, the initial position on the SOI (therefore, inclination of the parking orbit), the energy (therefore, eccentricity of the parking orbit), and the magnitude of the tangential periapsis departure burn were varied to match the outbound hyperbolic requirements.

Ascent and Descent for the MEM

In order to realistically model the effects of various Mars parking orbit strategies, ascent and descent trajectory simulations for the MEM were calculated for various inclinations and eccentricities. The propellant and tankage masses required for each of these cases were then included in the calculation of the entire interplanetary vehicle mass in LEO.

Descent

The descent was simulated as follows: a parking orbit was first established, then the descent to the surface was accomplished by separating the MEM from the main orbiter and performing a circularization burn at periapsis. Circularization of the MEM is desirable before deorbiting because the ΔV to deorbit is the same for any point in the circular orbit. This allows the MEM to descend to the northern as well as southern latitudes, and provides for day or night landing capability. Once circularization is complete, a deorbit burn is performed to initiate the entry and landing sequence. Deorbit ΔV values and the propellant usage were calculated using a Hohmann transfer from the current circular orbit to a transfer orbit with a vacuum periapsis of zero altitude. A 10-percent margin was included in all descent ΔV values.

Ascent

The ascent analysis was chosen to occur from the equator so rendezvous with the Mars orbiter can be accomplished over the entire range of inclinations considered in this study. A pitch rate steering guidance law was used to simulate the ascent trajectory (for a single-stage vehicle) to maximize the MEM mass inserted into a phasing orbit. Once in orbit (at this intermediate altitude), the MEM, using a Hohmann transfer, performed an apoapsis burn to achieve the parking orbit of the orbiter for rendezvous. The Martian atmosphere was modeled using the COSPAR northern hemisphere summer mean density. A 10-percent margin was also included in all ascent ΔV values.

Using the MEM characteristics shown in Table 2, a parametric study of inclination and eccentricity was performed, from which ascent and descent ΔV values were determined. The rocket equation was then used to obtain the mass of the MEM for the various inclinations and eccentric orbits.

Table 2
Mission Excursion Module Characteristics[8]

Initial dry mass	21,400 kg
Final dry mass	2,420 kg
Liftoff T/W (on Mars)	1.3
Liftoff T/W (on Earth	0.5
Reference diameter	9.754 m
Length of stopover	60 days
Crew	4
Isp_{vac}	360.5 sec

Gravity Model

The acceleration of a spacecraft acted upon by a central attracting body is

$$\frac{d^2\vec{r}}{dt^2} = \nabla U = \frac{\partial U}{\partial x}\vec{I} + \frac{\partial U}{\partial y}\vec{J} + \frac{\partial U}{\partial z}\vec{K}$$

where r is the position of the spacecraft and U is the gravitational potential.

The simplified gravitational potential for a spherically symmetric mass body is μ/r, which results in conic orbits. However, Mars is not spherically symmetric but is bulged at the equator and flattened at the poles, similar to Earth. Therefore, precession of a parking orbit results. To account for this nonuniform mass distribution, the following potential was used

$$U = \frac{\mu}{r}\left[1 - \sum_{n=2}^{\infty} J_n\left(\frac{r_e}{r}\right)^n P_n(\sin L)\right]$$

The above potential considers only the effects of the zonal harmonics (which are the dominant harmonics for Mars). These harmonics take into account the mass distribution which is symmetric about the north-south axis (i.e., they are latitude dependent only). The numerical values used in this analysis for Mars are

$\mu = 4.2828 \times 10^{13}\ m^3/sec^2$
$r_e = 3.40 \times 10^6\ m$
$J_2 = 1.9595 \times 10^{-3}$
$J_3 = 3.5837 \times 10^{-5}$
$J_4 = -1.1772 \times 10^{-5}$
$J_5 = 9.0793 \times 10^{-6}$
$J_6 = -3.1549 \times 10^{-7}$

Normalized zonal coefficients were obtained from Refs. 9, 10, and 11, averaged, and then converted by Kaula's rule of thumb [12] to produce the above actual values.

Computational Tools

The analysis in this study was initiated by determining inbound and outbound hyperbolic asymptotes with the Swingby-Stopover Optimization Program (SWISTO)[13], which uses a 3-dimensional patched conic approach. A candidate interplanetary trajectory was then selected and used as initial and final transfer orbit conditions. With these conditions, the orbital precession and ascent analyses were performed using the Program to Optimize Simulated Trajectories (POST).[14]

RESULTS AND DISCUSSION

Ascent and Descent of the MEM

Ascent and descent ΔV calculations for the MEM are shown in Figures 2 through 4 for periapsis altitudes of 500 km and 250 km. Figure 2 shows that there is a near linear variation in descent ΔV with eccentricity. That is, the more eccentric the parking orbit, the greater the descent ΔV required. Figures 3 and 4 show the influence of inclination for the various eccentricities on the required ascent ΔV. With these ΔV values and the characteristics in Table 2, MEM masses were calculated and are shown in Figs. 5 and 6. As seen in Figs. 3 and 4, a maximum penalty of about 0.6 km/sec is imposed on a due westward launch when compared

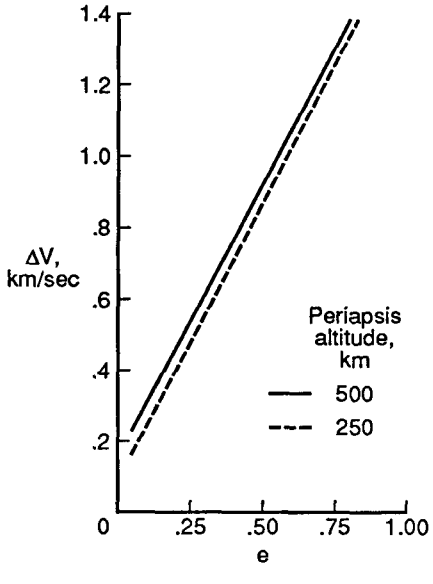

Fig. 2 MEM descent ΔV.

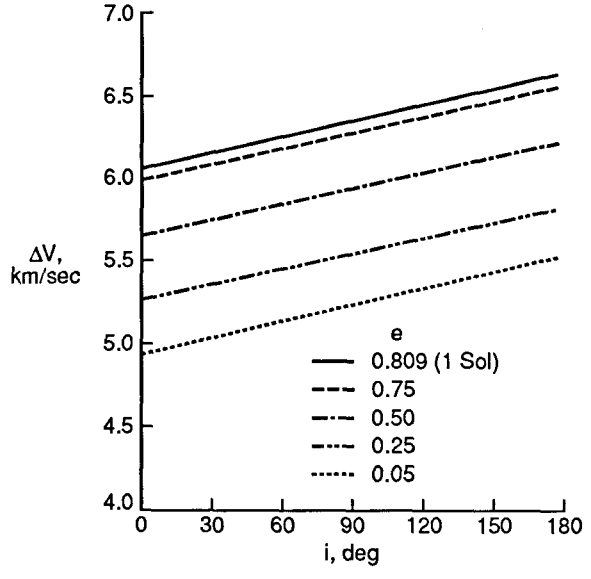

Fig. 3 MEM ascent ΔV for a periapsis altitude of 500 km.

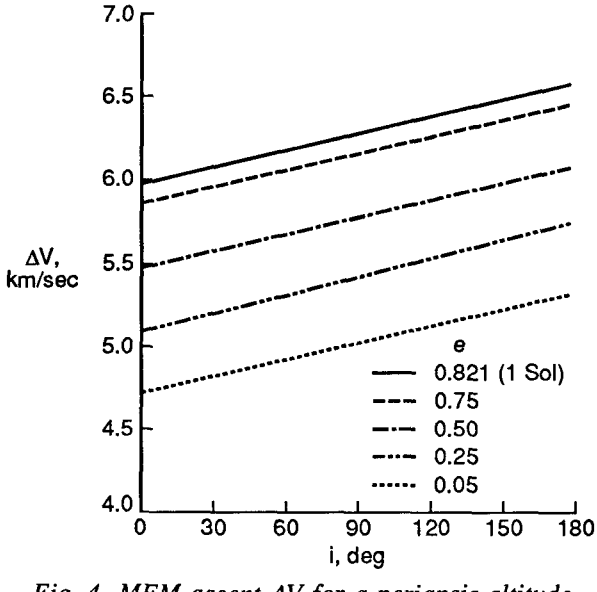

Fig. 4 MEM ascent ΔV for a periapsis altitude of 250 km.

with a due eastward launch. This translates into a maximum increase of about 13,500 kg in the MEM mass (for the 1 Sol orbit) as shown in Figs. 5 and 6. As seen from the figures, inclination does have some impact on the mass of the MEM. However, as shown later, this impact is insignificant compared with the overall mass of the entire vehicle in low-Earth orbit. In fact, the departure ΔV is the main driver in determining the parking orbit. Therefore, the consideration of a parking orbit need not be limited to direct orbits only

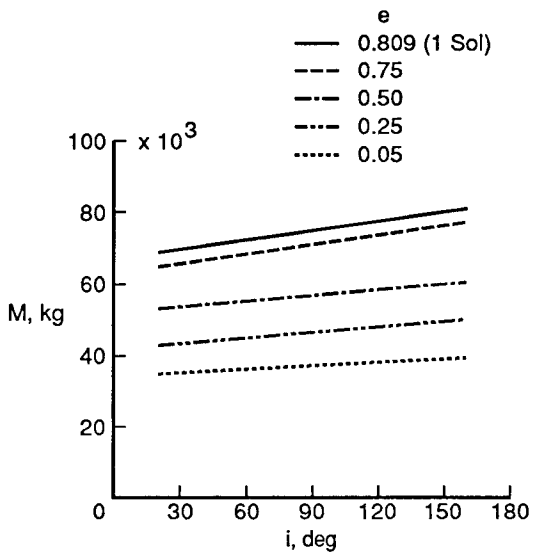

Fig. 5 MEM mass for a periapsis altitude of 500 km.

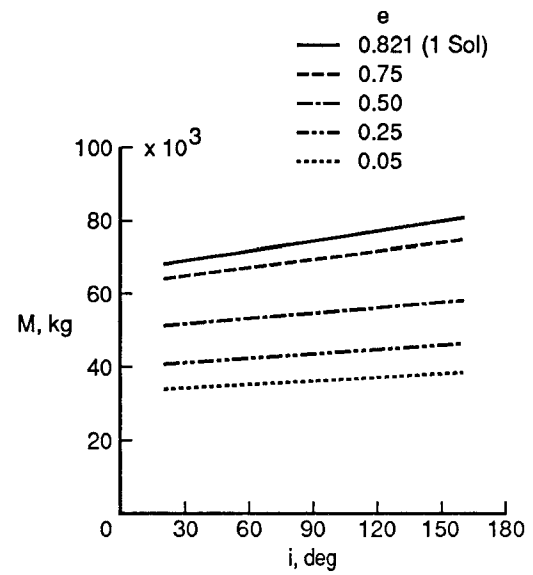

Fig. 6 MEM mass for a periapsis altitude of 250 km.

and should be expanded to include retrograde orbits. The figures also show that periapsis altitude does not affect either the ΔV values or the MEM mass significantly.

Parametric Study

Figs. 7 through 12 show the vehicle mass ratio (M_i/M_f) versus inclination for various eccentricities. One clarification needs to be made about Figs. 7 through 12. The curves displayed are the best possible match to the data. For the higher eccentricities, continuous curves are shown. However, for the low eccentric orbits, only computed points are displayed because exact curve fits were not possible due to the random or "scatter-like" behavior that is observed. This behavior is due to the high rate of precession encountered at low eccentricities. As a result, a drastic change in the departure geometry is seen for slight changes in inclination.

Figs. 7 and 8 show a large variation in M_i/M_f for a periapsis departure for the parking orbits considered. As seen, certain combinations of the orbital parameters (especially those with low eccentricity) induce a drastic M_i/M_f penalty. Ranges in M_i/M_f of about 150 to 1900 are seen for the two periapsis altitudes. This suggests that periapsis (true anomaly = 0°) may not be the optimum location for departure. Therefore, the analysis was repeated to determine the effect of true anomaly upon minimizing the departure ΔV (hence, M_i/M_f).

The results from an optimization of true anomaly are shown in Figs. 9 and 10. As seen from these figures, M_i/M_f has been drastically reduced from an initial range of 150-1900 to a new range of 140-450, and indeed periapsis is not the best location for departure for a majority of the orbits. However, in the search for a optimal departure location, an optimization problem within POST was encountered. That is, many local optimums complicated the search for the departure true anomaly which resulted in a minimum departure ΔV. Therefore, a global optimum was not always guaranteed. Fig. 11 shows this effect for the e = 0.75 curve from Fig. 9. The analysis was repeated for the first two points (i = 21.5° and 40°) using different initial conditions. This produced much lower mass ratios, and hence, a more optimum departure location or true anomaly was obtained. To obtain exact and precise plots of M_i/M_f, a parametric study in true anomaly must also be performed along with inclination and eccentricity in order to determine the minimum

departure ΔV. However, this is a very tedious and time consuming process.

In order to obtain a more exact trend of how these orbits behave, a parametric study in true anomaly was performed for three inclinations (i = 21.5°, 90°, 158.5°) for the 1 Sol parking orbit with a periapsis altitude of 500 km. Fig. 12 compares the results for periapsis departure (from Fig. 7) with those for an optimized departure location. As seen, a penalty is imposed for departure from periapsis for this mission profile. The size of this penalty depends upon the inclination of the orbit. In this case, a large penalty in M_i/M_f is imposed for inclinations less than 90°, and in fact, periapsis is not the optimum location for departure for most orbits.

Figure 12 also shows that for the optimized departure curve, lower values of M_i/M_f are obtained for orbits with equatorial inclinations (i.e., at very low or high inclination). As a result, these orbits look very favorable from a mission performance (M_i/M_f) point of

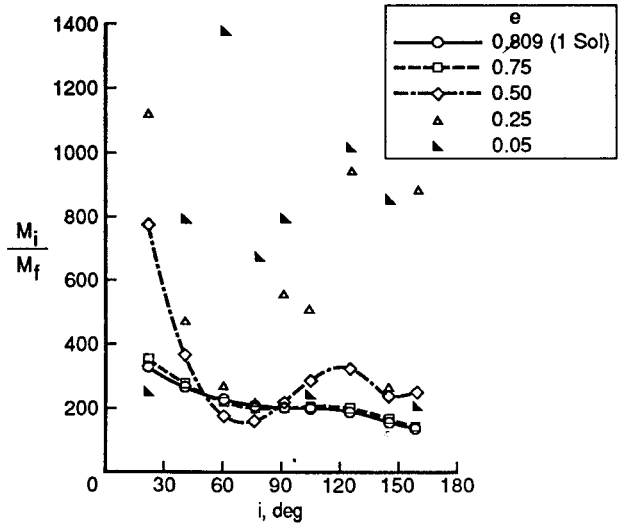

Fig. 7 Mass ratio in LEO with a periapsis departure (periapsis altitude = 500 km).

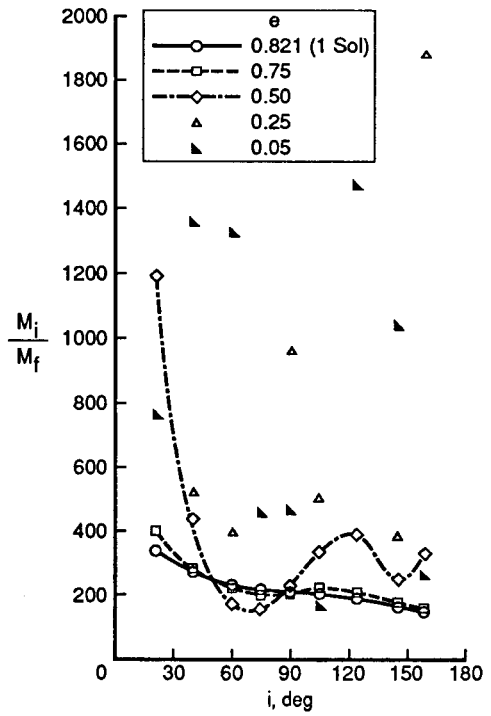

Fig. 8 Mass ratio in LEO with a periapsis departure (periapsis altitude = 250 km).

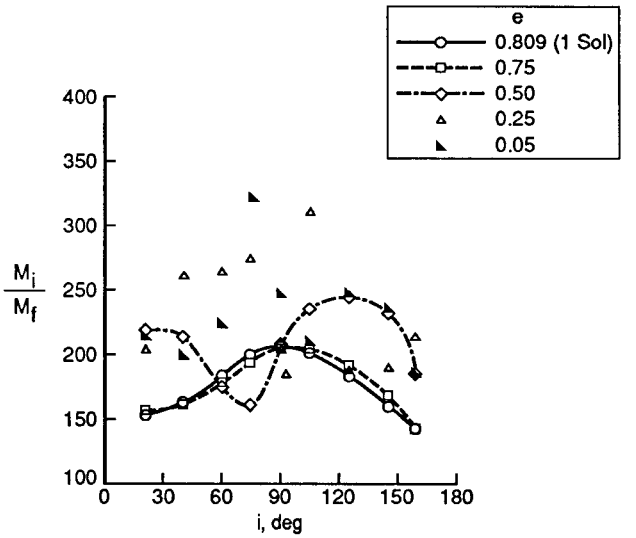

Fig. 9 Mass ratio in LEO with an optimized departure (periapsis altitude = 500 km).

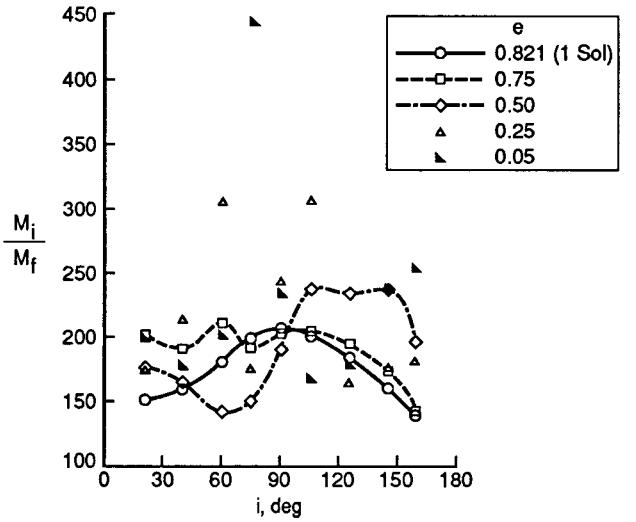

Fig. 10 Mass ratio in LEO with an optimized departure (periapsis altitude = 250 km).

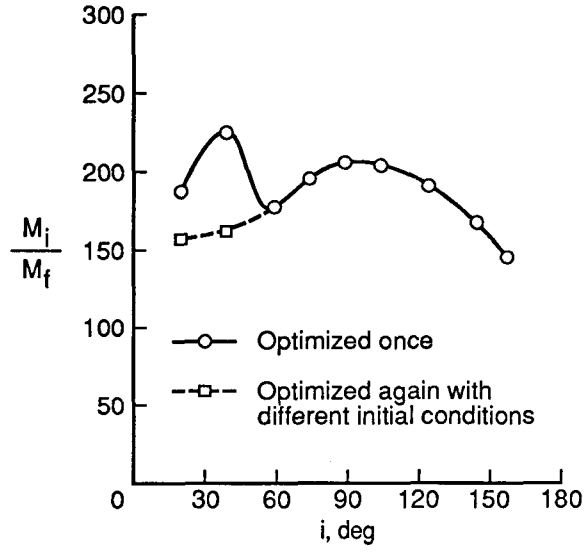

Fig. 11 Change in M_i/M_f caused by local optimums (periapsis altitude = 500 km, eccentricity = 0.75).

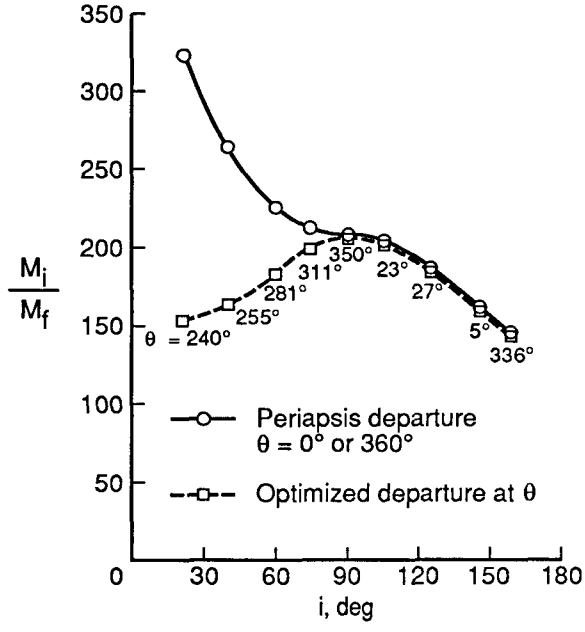

Fig. 12 Comparison of M_i/M_f in LEO between a periapsis departure and an optimized departure location (periapsis altitude = 500 km, eccentricity = 0.809)

view. However, because of their limited planetary coverage, equatorial orbits display poor characteristics for scientific observations and landing site accessibility. Therefore, if a non-equatorial orbit is required to improve the scientific and landing site requirements, a penalty in mission performance (M_i/M_f) is induced. For example, to achieve a polar orbit, an increase in M_i/M_f of 46.1 percent is required as seen in Fig. 12.

In summary, a few general statements concerning parking orbit selection can be made from these parametric results (1) Periapsis altitude does not have a major impact on M_i/M_f as seen in Figs. 9 and 10. Most values of M_i/M_f are in the range from 150 to 300 for both altitudes. Since a variation in M_i/M_f is present, the choice of a parking orbit cannot be made arbitrarily, and a thorough analysis is required to minimize the initial LEO mass. (2) No one particular eccentricity is favorable for the entire range of inclinations. In fact, a low eccentricity (e = 0.50) is favored over a high eccentricity (e = 0.75 or 1 Sol orbit) for intermediate inclinations (i ≈ 45° to 85°) for both periapsis altitudes. (3) Periapsis is not the optimum location for departure for a majority of the orbits as shown in Fig. 12. (4) Also from Fig. 12, a retrograde orbit (i = 158.5°) can result in a lower M_i/M_f than a direct orbit (i = 21.5°). Therefore, the increase in the MEM mass associated with retrograde orbits should not be an issue for parking orbit selection.

Exact Precession Study

One way of minimizing the penalty in mission performance, while still achieving scientific requirements, is to search for an exact precession parking orbit, that is, a parking orbit which precesses in such a way that a tangential periapsis departure burn can be performed at the end of the stopover; thereby, reducing the departure ΔV.

From this study, it was determined that only a finite number of exact precession orbits exist. The problem arises in that an alignment of the argument of periapsis, the longitude of ascending node, and true anomaly is necessary before a tangential burn can be performed at periapsis for departure. Since these parameters precess at different rates, there are only a few combinations of these parameters which result in a tangential periapsis departure burn for a given stopover time and periapsis altitude. In this study, nine exact precession orbits were found, five for a periapsis altitude of 500 km and four for a periapsis altitude of 250 km (for this interplanetary mission profile). Tables 3 and 4 list the various characteristics of these orbits and other orbits of interest for the two periapsis altitudes. Note that the orbits are numbered for reference.

Comparison of these different orbits shows that exact precession orbits can result in minimum M_i/M_f. However, for this mission profile, an exact precession

Table 3
Potential Parking Orbits for a Periapsis Altitude of 500 km

	Parking Orbit Number	Parking Orbit Characteristics	$\Delta V_{ins.}$, km/sec	$\Delta V_{dept.}$, km/sec	Departure Burn Direction	Mass Ratio in LEO, M_f/M_i	Mass in LEO, kg x 10^6
Exact Precession	1	i = 70.7°, e = 0.381	3.28	2.18	Tangential θ = 0°	145.3	0.9880
	2	i = 135.7°, e = 0.225	3.51	2.43	Tangential θ = 0°	155.9	1.060
	3	i = 51.5°, e = 0.0992	3.71	2.63	Tangential θ = 0°	162.9	1.108
	4	i = 133.7°, e = 0.0358	3.81	2.71	Tangential θ = 0°	170.1	1.157
	5	i = 129.2°, e = 0.0125	3.85	2.76	Tangential θ = 0°	172.1	1.170
3-dimen-sional	6	i = 158.5°, e = 0.809	2.72	1.66	γ = 6.3° β = 6.4° θ = 336°	141.5	0.9622
	7	i =21.5°, e = 0.809	2.72	2.69	γ = 29.4° β = 212.4° θ = 240°	152.9	1.040
	8	i =75°, e = 0.809	2.72	3.67	γ = 17.8° β = 81.4° θ = 281°	182.8	1.243
	9	i =90°, e = 0.809	2.72	4.25	γ = 26.5° β = 91.8° θ = 350°	206.7	1.406

Table 4
Potential Parking Orbits for a Periapsis Altitude of 250 km

	Parking Orbit Number	Parking Orbit Characteristics	$\Delta V_{ins.}$, km/sec	$\Delta V_{dept.}$, km/sec	Departure Burn Direction	Mass Ratio in LEO, M_f/M_i	Mass in LEO, kg x 10^6
Exact Precession	1	i = 71.1°, e = 0.436	3.18	2.10	Tangential θ = 0°	138.9	0.9445
	2	i = 21.6°, e = 0.1684	3.58	2.50	Tangential θ = 0°	155.1	1.055
	3	i = 105.3°, e = 0.053	3.77	2.71	Tangential θ = 0°	166.2	1.130
	4	i = 1 19°, e = 0.005	3.85	2.75	Tangential θ = 0°	168.3	1.144
3-dimen-sional	5	i = 158.5°, e = 0.821	2.66	1.65	γ = 8.5° β = 9.6° θ = 330°	138.8	0.9438
	6	i =21.5°, e = 0.821	2.66	2.71	γ = 149.8° β = 201.9° θ = 236.9°	150.7	1.025
	7	i =75°, e = 0.821	2.66	4.18	γ = 21.9° β = 90.7° θ = 310°	199.0	1.353
	8	i =90°, e = 0.821	2.66	4.36	γ = 27.6° β = 93.2° θ = 351°	207.6	1.412

orbit was not found to yield the lowest mass ratio. Therefore, from these results, an exact precession orbit should not be selected if minimizing the M_i/M_f is the main objective of the mission. For this interplanetary mission profile, a 1 Sol orbit with an inclination of 158.5° and requiring a three-dimensional departure burn yields the minimum M_i/M_f for either periapsis altitude. However, being near-equatorial, these orbits are very poor from a scientific standpoint and limit the choice of potential landing sites. Therefore, a penalty in mission performance is required to obtain a more favorable inclination for these science requirements. In comparison to the i = 158.5°, e = 1 Sol orbit, Figs. 13 and 14 show the percent increase in M_i/M_f required for

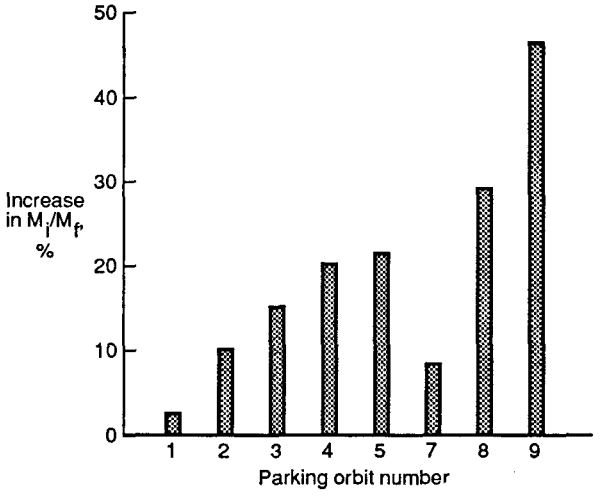

Fig. 13 Percent increase in M_i/M_f for various parking orbits with a periapsis altitude of 500 km.

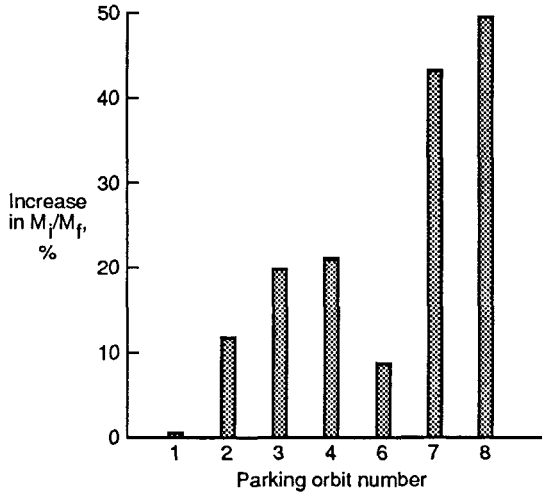

Fig. 14 Percent increase in M_i/M_f for various parking orbits with a periapsis altitude of 250 km.

achieving the various parking orbits from Tables 3 and 4 for the two periapsis altitudes. For example, to achieve a more favorable inclination, an increase in M_i/M_f of 46.1 percent (orbit no. 9 from Fig. 13) and 49.6 percent (orbit no. 8 from Fig. 14) is imposed for achieving a polar orbit for periapsis altitudes of 500 km and 250 km, respectively.

The advantages of using exact precession orbits are that lower eccentricities and more favorable inclinations are possible without a drastic penalty in mission performance. Penalties of only 2.7 percent and 0.07 percent in M_i/M_f are required for the exact precession orbits with i = 70.7°, e = 0.381, altp = 500 km (orbit no. 1 from Fig. 13) and i = 71.1°, e = 0.436, altp = 250 km (orbit no. 1 from Fig. 14), respectively. To obtain a comparable inclination (i = 75°) for the 1 Sol orbits, increases of 29.2 percent (orbit no. 8 from Fig. 13) and 43.3 percent (orbit no. 7 from Fig. 14) in M_i/M_f are required for periapsis altitudes of 500 km and 250 km, respectively.

Therefore, if arrival characteristics (inclination and eccentricity) of the parking orbit are allowed to vary rather than arbitrarily selecting them as in the parametric study, favorable departure conditions (i.e., a tangential periapsis departure burn) can be obtained, resulting in lower M_i/M_f penalties. Hence, in general by choosing exact precession orbits, global scientific observations and candidate landing sites can be increased without sacrificing mission performance significantly.

CONCLUSIONS

This investigation was initiated to identify trends and aspects of Mars parking orbits for an initial manned mission. Based on this analysis pertaining to the following mission profile

Earth departure:	April 5, 2017
Venus swingby:	September 10, 2017
Mars arrival:	March 24, 2018
Mars departure:	May 23, 2018
Earth return:	November 15, 2018

with Earth departure and return ΔV values of 4.17 km/sec and 1.13 km/sec, respectively, and inbound and outbound interplanetary velocity vectors of

Inbound	Outbound
$\alpha = 253.99°$	$\alpha = 212.57°$
$\delta = -21.4°$	$\delta = -12.5°$
$\lvert\vec{V}_\infty\rvert = 5.441$ km/sec	$\lvert\vec{V}_\infty\rvert = 3.873$ km/sec

many general statements can be made.

(1) Precession has a drastic effect on departure ΔV, and hence, on the mass ratio in LEO. Therefore, the choice of a parking orbit cannot be made arbitrarily, and a detailed analysis must be performed to obtain an optimum parking orbit.

(2) Both the MEM mass and the overall vehicle mass in LEO are insensitive to periapsis altitude.

(3) True anomaly must be considered along with inclination and eccentricity in determining the minimum departure ΔV, and hence, the initial minimum LEO mass.

(4) The choice of parking orbit inclination should not be limited to direct orbits only. Retrograde orbits can result in lower M_i/M_f, even with the increase in MEM mass associated with their use.

(5) Higher eccentricities (e.g., 1 Sol orbit) do not necessarily imply minimum mass ratios. For some inclinations, a lower eccentricity is favored.

(6) The minimum initial LEO mass was obtained for a highly eccentric parking orbit which did not precess exactly and required a three-dimensional departure burn. Therefore, a three-dimensional departure burn need not imply mission inefficiency.

(7) To enhance science requirements, a penalty in mission performance (M_i/M_f) may be imposed. This penalty can be minimized by using an exact precession orbit.

(8) The advantage of utilizing an exact precession orbit, in comparison with an orbit which is chosen arbitrarily requiring a three-dimensional departure burn, is that lower eccentricities and more favorable inclinations (i.e., better scientific requirements) are obtainable without significantly increasing initial LEO mass (i.e., decreasing mission performance). For this mission profile, exact precession orbits were not found to yield the lowest mass ratio. However, they may for other manned Mars mission profiles.

In summary, a trade-off between mission performance, scientific observations, and landing site accessibility must be made in the selection of a parking orbit.

ACKNOWLEDGMENTS

The authors would like to extend their thanks to the people who helped guide this study. In particular, the comments and suggestions of Richard Powell, James Buglia, and Robert Tolson of the Langley Research Center and Dr. Gerald Walberg of The George Washington University were always helpful. Additionally, thanks should be extended to Anne Costa who has helped produce this report. Support for this investigation has been provided through Cooperative Research Agreement NCC1-104 from NASA Langley Research Center. This research is a portion of the material to be included in a forthcoming Master of Science thesis with The George Washington University.[15]

REFERENCES

[1]Braun, R.D., "The Influence of Interplanetary Trajectory Options on a Chemically Propelled Manned Mars Vehicle," The Journal of Astronautical Sciences, Vol. 38, No. 3, July - September 1990.

[2]Woodcock, G.R.; "Analysis of Technologies for Manned Lunar and Mars Missions," Final Technical Report, Contract NAS8-36107, Huntsville, Alabama, April 1989.

[3]Young, A.C.; Mulqueen, J. A.; and Skinner, J.E., "Mars Exploration Venus Swingby and Conjunction Class Mission Modes Time Period 2000 to 2045," NASA TM-86477, August 1984.

[4]Babb, G.R. and Stump, W.R., "Mars Orbit Selection," Manned Mars Mission Conference, NASA TM 89320, June 1986.

[5]Tucker, M.; Meredith, O.; and Brothers, B., "Space Vehicle Concepts," Mars Mission Conference, NASA TM 89320, June 1986.

[6]Walberg, G.D., "A Review of Aerobraking for Mars Missions," IAF Paper No. 88-196, October 1988.

[7]Tolson, R.H., "Geometrical Characteristics of Lunar Orbits Established from Earth-Moon Trajectories," NASA TN D-1780, April 1963.

[8]Stump, W.R.; Babb, G.R.; and Davis, H.P., "Mars Lander Survey," Manned Mars Mission Conference, NASA TM 89320, June 1986.

[9]Christensen, E.J. and Balmino, G., "Development and Analysis of a Twelfth Degree and Order Gravity Model for Mars," Journal of Geophysical Research, Vol. 84, No. B14, December 1979.

[10]Gapcynski, J.P.; Tolson, R.H.; and Michael, W.H. Jr., "Mars Gravity Field: Combined Viking and Mariner 9 Results," Journal of Geophysical Research, Vol. 82, No. 28, September 1977.

[11]Daniels, E.F.; Tolson, R.H.; and Gapcynski, J.P., "Spherical Harmonic Representation of the Martian Gravity Using a Short-Arc Technique," Journal of Spacecraft and Rockets, Vol. 14, No. 6, June 1977.

[12]Kaula, W.M., Theory of Satellite Geodesy: Application of Satellites to Geodesy, Blaisdell Publishing Co., 1966.

[13]Mead, C.W. and Jones, M.F., "Optimization of Ephemeridal Parameters for Minimum Propellant Requirements on Multiplanet Roundtrip Swingby-Stopover Missions," Final Technical Report, Contract NAS8-20082, LMSC Huntsville Research & Engineering Center, May 1968.

[14]Brauer, G.L.; Cornick, D.E.; and Stevenson, R., "Capabilities and Applications of the Program to Optimize Simulated Trajectories (POST)," NASA CR-2770, February 1977.

[15]Desai, P.N., "Aspects of Parking Orbit Selection in a Manned Mars Mission," Masters Thesis, The George Washington University/JIAFS Program, August 1990.